Available online at www.sciencedirect.com
ScienceDirect
Journal of the European Ceramic Society 30 (2010) 2671–2676
www.elsevier.com/locate/jeurceramsoc

Processing of microcellular silicon carbide ceramics with a duplex pore structure

In-Hyuck Song [a,*], Il-Min Kwon [a], Hai-Doo Kim [a], Young-Wook Kim [b]

[a] Engineering Ceramics Group, Korea Institute of Materials Science, 531 Changwondaero, Changwon, Gyeongnam 641-831, Republic of Korea
[b] Department of Materials Science and Engineering, The University of Seoul, Dongdaemoon-ku, Seoul 130-743, Republic of Korea

Received 25 October 2009; received in revised form 6 April 2010; accepted 23 April 2010
Available online 18 May 2010

Abstract

A novel processing route for producing microcellular SiC ceramics with a duplex pore structure has been developed using a polysiloxane, carbon black, SiC, Al_2O_3, Y_2O_3, and two kinds of pore former (expandable microspheres and PMMA spheres). The duplex pore structure consists of large pores derived from the expandable microspheres and small windows in the strut area that were replicated from the PMMA spheres. The presence of these small windows in the strut area improved the permeability of the porous ceramics. The gas permeability coefficients of porous SiC ceramics were 0.13×10^{12} m^2 for the porous SiC without PMMA spheres, 0.47×10^{12} m^2 for the porous SiC with 10 wt% PMMA spheres, and 0.82×10^{12} m^2 for the porous SiC with 20 wt% PMMA.

Keywords: SiC; Porosity; Permeability; Foaming; Polysiloxane

1. Introduction

Porous ceramics have been widely used as filters, membranes, catalytic substrates, thermal insulation, gas-burner media, and refractory materials, owing to their superior properties, such as low bulk density, high permeability, high temperature stability, erosion/corrosion resistance, and excellent catalytic activity.[1–6] The performance of porous ceramics greatly depends on pore morphology, size, and distribution; these factors, in turn, are determined by the processing steps involved in the fabrication of ceramic foams. Efforts to produce porous ceramics with improved performance have led to the development of several processing techniques.

Ceramic foams can be fabricated by a variety of methods, including replication,[7–11] sacrificial template,[12–18] and direct foaming approaches.[19–26] Recently, three different processing strategies for fabricating microcellular ceramics with cell densities of $>10^9$ cells/cm^3 and cells of $<50\,\mu$m have been developed. The first strategy involves saturating preceramic polymers using gaseous, liquid, or supercritical CO_2; nucleating and growing a large number of bubbles using thermodynamic instability by a rapid pressure drop or heating; and transforming the microcellular preceramics into microcellular ceramics by pyrolysis and optional subsequent sintering.[27,28] The second strategy involves forming certain shapes using a mixture of preceramic polymer and expandable microspheres; foaming and cross-linking the compact by heating; and transforming the foamed preceramics into microcellular ceramics by pyrolysis.[29,30] The third strategy involves simple pressing of a silicone resin powder mixed with polymer microbeads as sacrificial templates.[31,32]

Porous silicon carbide (SiC) ceramics show unique characteristics such as low density, low thermal conductivity, controlled permeability, high thermal shock resistance, high surface area, and high specific strength, which usually cannot be achieved in their conventional dense counterparts. On these bases, they have found many applications including filtration of molten metal, filtration of particles from diesel engine exhaust gases, filtration of hot corrosive gases in various industrial applications, gas-burner media, membrane supports for hydrogen separation and lightweight structural parts for high temperature applications.[33–36] For filters, vacuum chucks, and air spindle applications, the achievement of high gas permeability is a key factor in the development of porous SiC ceramics. However, very few reports on

* Corresponding author. Tel.: +82 55 280 3534; fax: +82 55 280 3399.
E-mail address: sih1654@kims.re.kr (I.-H. Song).

0955-2219/$ – see front matter.
doi:10.1016/j.jeurceramsoc.2010.04.027

Table 1
Batch compositions of porous SiC ceramics.

Sample	Batch composition (wt%)					
	Polysiloxane	Carbon	SiC	Expandable microsphere	PMMA	Sintering additive
P0	30	3	57	10	0	$3.8Y_2O_3 + 8.8Al_2O_3$
P1	30	3	47	10	10	$3.1Y_2O_3 + 7.2Al_2O_3$
P2	30	3	37	10	20	$2.5Y_2O_3 + 5.8Al_2O_3$

the gas permeability of porous SiC ceramics can be found in the literature.

In this paper, porous SiC ceramics were fabricated by carbothermal reduction of a polysiloxane-derived SiOC and a subsequent sintering process. In particular, two kinds of pore formers, expandable microspheres and PMMA spheres, were added simultaneously to create a duplex pore structure with high permeability. The effects of PMMA sphere content on porosity and permeability were investigated.

2. Experimental procedure

The raw materials used included: a polysiloxane (polymethylsiloxane, YR3370, density = 1.036 g/cm^3, GE Toshiba Silicones Co., Ltd., Tokyo, Japan), a carbon black (Corax MAF, Korea Carbon Black Co., Ltd., Inchon, Korea), SiC (UF 15, H. C. Starck, Germany), Al_2O_3 (AKP30, Sumitomo Chemical Co., Tokyo, Japan) and Y_2O_3 (grade C, H. C. Starck, Germany). SiC was added as inert filler and Al_2O_3 and Y_2O_3 were added as sintering additives. Two kinds of pore formers: expandable microspheres (461DU40, Expancel, Sundsvall, Sweden) and PMMA sphere (particle size 8 μm, Sunjin, Korea), were used to make a duplex pore structure. Three batches of powder were prepared and the content of the PMMA in those batches ranged from 0 wt% to 20 wt% (Table 1). The expandable microspheres consist of a thermoplastic (poly(methyl methacrylate)) shell that encapsulates a hydrocarbon gas. Heating the microsphere increases the pressure of gas inside it, and the thermoplastic shell softens, resulting in increased volume of the microspheres. Ethanol was used as a solvent for homogeneous mixing of the polysiloxane with other raw materials, because the polysiloxane is soluble in ethanol. The slurry was dried and sieved through a 250 mesh screen. The mixed powders were placed in a mold with an internal volume of 64 cm^3 (8 cm × 8 cm × 1 cm). The powders were expanded in an oven, where the sample was heated up to 140 °C in air at a heating rate of 2 °C/min. When heated, the microspheres expanded and the polysiloxane softened, resulting in an increase of the foam volume to the mold volume. The expanded foams were cross-linked by heating them up to 180 °C in air. The cross-linked samples were pyrolyzed at 1200 °C for 1 h with a heating rate of 1 °C/min in argon. The heat-treatment allows for the conversion of polysiloxane to silicon oxycarbide in the specimens. The pyrolyzed specimens were further heat-treated in argon at 1450 °C for 1 h with a heating rate of 10 °C/min and subsequently sintered at 1750–1850 °C for liquid-phase sintering of SiC using Al_2O_3 and Y_2O_3. The bulk density of the microcellular ceramics was computed from the weight-to-volume ratio of the samples. The total porosity of the porous ceramics was calculated from the bulk density of the microcellular ceramic and the theoretical density of SiC. The open porosity and pore size distribution was measured using a mercury porosimeter (AutoPore IV9500 v1.04, Micromeritics Instrument Corporation). Mercury is a nonwetting liquid for SiC. Thus, it does not flow spontaneously into the pores of the present specimens. Pressure was applied on mercury in order to intrude it into the pores. Pore diameter was obtained using equation ($D = -4\gamma \cdot \cos\theta/\Delta p$, where D is pore diameter, γ and θ are surface tension and contact angle, respectively, of the liquid, and Δp is differential pressure).[37] Permeability was measured by a Capillary Flow Porometer (CFP-1100-AEX, PMI). The gas permeability coefficient (α) was computed from the measured flow rate and pressure difference using Darcy's law ($\Delta p/e = Q \cdot \eta/A \cdot \alpha$, where Δp is pressure difference, e is thickness, Q is flow rate, η is viscosity of the fluid, A is cross-sectional area, and α is the permeability coefficient).[37]

3. Results and discussion

The general reaction for synthesizing SiC from a mixture of polysiloxane and carbon black has been reported in a previous paper.[38] The reaction occurs in two steps: (i) the pyrolysis of polysiloxane at 1200 °C, which involves the loss of organic materials and also leads to the conversion of polysiloxane to SiOC; and (ii) the carbothermal reduction of the SiOC and C mixture at 1450 °C, which converts the mixture to a SiC ceramic with evolution of gaseous CO. Sintering of the SiC synthesized by the carbothermal reduction and added as an inert filler was achieved at 1800–1950 °C with the addition of Al_2O_3–Y_2O_3. It was also reported that pyrolysis of the polysiloxane in an inert atmosphere yielded SiOC, with a weight loss of 13% and the carbon content of the polysiloxane-derived SiOC was 11.5%.[30] This residual carbon and additionally added carbon were the sources of the carbothermal reduction for conversion to SiC.

Fig. 1 shows the density changes according to the stages of the processing procedure: as-foamed, as-cross-linked, as-pyrolyzed (1200 °C for 1 h), and as-sintered specimens (1800 °C for 3 h) including 1 h hold at 1450 °C for carbothermal reduction during heating to the sintering temperature. The specimen with 20 wt% PMMA (P2) showed higher density than the others after foaming, because the addition of more PMMA decreased the expansion ratio. It is speculated that the addition of same weight to fixed volume resulted in higher volume loading of the P2 specimen than the others due to the lower density of PMMA relative to SiC filler. There was no change in the specimen

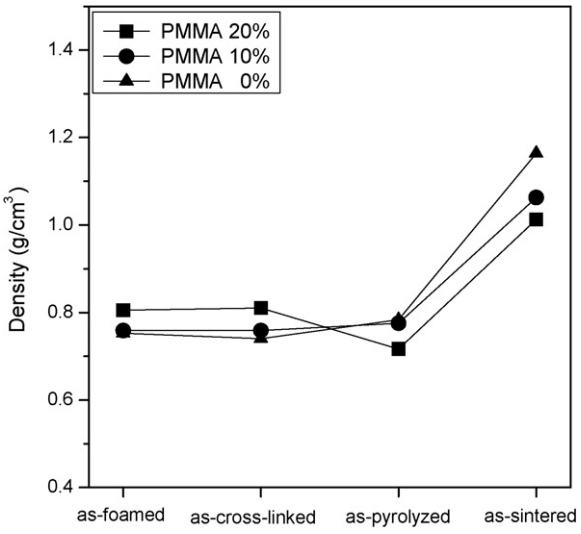

Fig. 1. Density changes according to the stages of the processing procedure: as-foamed, as-cross-linked, as-pyrolyzed, and as-sintered specimens (1800 °C for 3 h).

density after cross-linking due to the near absence of volume and weight changes. However, the density of P2 decreased, ultimately reaching the lowest value among all specimens, after the pyrolysis step, because of severe weight loss from the specimen. The weight loss originated from the decomposition of organic materials such as expandable microspheres, PMMA spheres, and polysiloxane. Since P2 contained the largest amount of organics, it is reasonable that the density became the lowest. The volume shrinkage of the P2 specimen was roughly 10% during the pyrolysis process. After carbothermal reduction and sintering processes, the density of all specimens increased due to densification of the strut by liquid-phase sintering with Al_2O_3 and Y_2O_3. After sintering, P0 showed the highest density (1.16 g/cm^3) and P2 the lowest (1.01 g/cm^3), because the sinterability of each specimen was dependent on the density after pyrolysis.

Fig. 2 shows the microstructures after pyrolysis, which was carried out at 1200 °C for 1 h. The specimen without PMMA (P0) (Fig. 2(a)) showed a typical cellular structure without secondary pores. In contrast, the specimen with 20% PMMA (P2, Fig. 2(b)) showed a duplex pore structure, where large pores replicated from expandable microspheres and small pores from PMMA spheres. The number of small pores increased as the PMMA content was increased.

Fig. 3 shows the effect of PMMA content on sintered density of porous SiC ceramics with variation of sintering temperature and porosity variation of SiC ceramics sintered at 1750 °C for 3 h. As shown in Fig. 3(a), the sintered density of SiC ceramics decreased with increasing PMMA content due to the increase of total pore former content. The density of the SiC ceramics increased with increasing sintering temperature due to the increased densification at higher temperatures. The present results suggest that the density of porous SiC ceramics can be controlled to some extent by adjusting the sintering temperature. Fig. 3(b) shows total and open porosities of the microcellular SiC ceramics sintered at 1750 °C for 3 h as a function of the PMMA content. The cumulative pore volume obtained by intrusion measurements using a mercury porosimeter indicates the open porosity. It can be seen that the total porosity and open porosity increased with increased PMMA content. However, the difference between total porosity and open porosity, which means the closed pore, decreased with increasing the PMMA content. It clearly suggests that the addition of PMMA spheres is beneficial for decreasing the closed porosity. The closed porosity would constrain the permeability of the samples. P2 specimen which contained 20% PMMA has almost no closed porosity, suggesting better permeability than the other specimens.

Fig. 4 shows the microstructures of porous SiC ceramics, without and with PMMA spheres, sintered at 1850 °C for 3 h. There is no difference in the large cell size and cell density between (a) and (b) of Fig. 4 when only large cells are counted, suggesting the cells replicated from the expandable microspheres. The apparent cell size of the large pores was 12.4 ± 5.3 μm for both specimens, and the maximum cell sizes ranged from 35 μm to 45 μm for both specimens. Typical cell densities of large pores were $\sim 1.0 \times 10^9$ cells/cm^3 for both specimens. However, with the addition of PMMA sphere (Fig. 4(b)), the strut microstructure has been changed from a partially interconnected structure to a pore structure with many small openings. Small PMMA particles (8 μm) created an opening in the strut and produced the secondary pore structure. Evidently, the large pores derived from the expandable microspheres and the small pores in the strut derived from the PMMA spheres.

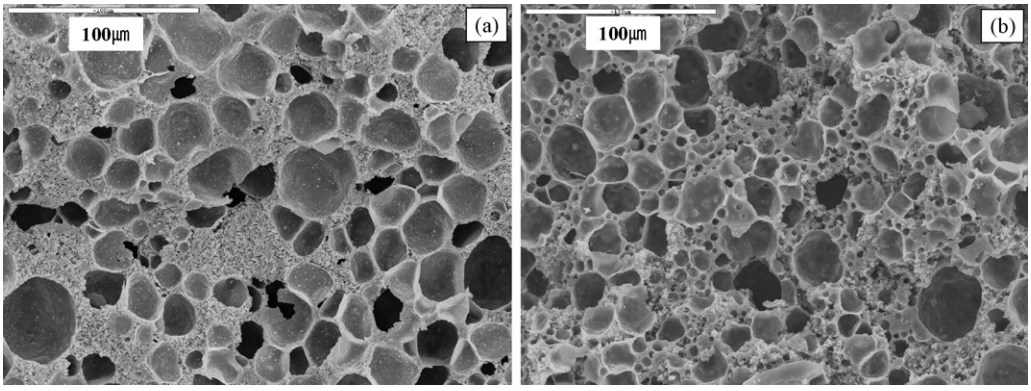

Fig. 2. Microstructure after pyrolysis at 1200 °C for 1 h: (a) P0 (0 wt% PMMA) and (b) P2 (20 wt% PMMA).

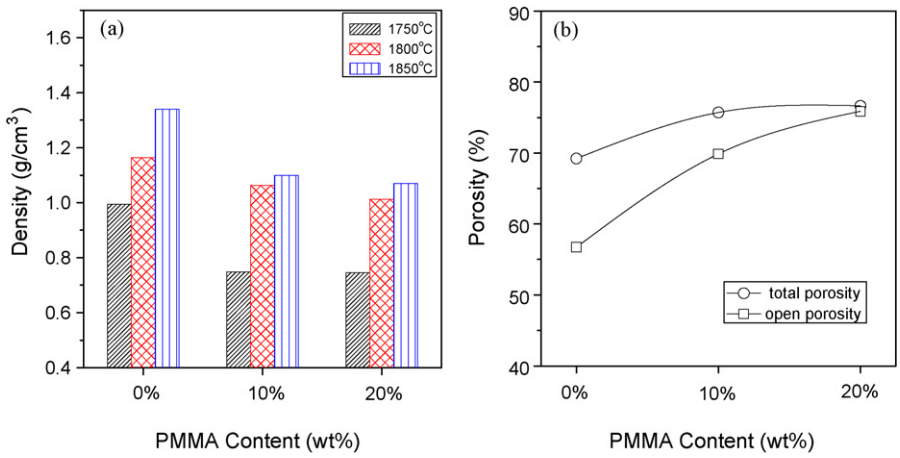

Fig. 3. Effect of PMMA content on (a) sintered density of porous SiC ceramics with variation of sintering temperature and (b) porosity variation of SiC ceramics sintered at 1750 °C for 3 h.

The present results suggest that the addition of two different sizes of templates is an efficient way to control the openness of the strut.

Fig. 4(c), a higher magnification micrograph of Fig. 4(b), shows that the strut consists of small equiaxed grains (1–2 μm in diameter). The strut microstructure is the same as the microstructure of liquid-phase sintered SiC sintered at the same temperature,[39] indicating that SiC was successfully synthesized from polysiloxane and carbon as a result of carbothermal reduction, and was sintered with Al_2O_3 and Y_2O_3 by the subsequent sintering process.

Fig. 5 shows the pore size distribution of porous SiC ceramics sintered at 1850 °C for 3 h. According to the results, the average pore size increased from about 3 μm for the P0 specimen to 7 μm for the P2 specimen. The pore size is the secondary pore size in the strut. The primary pores replicated from expandable microspheres were not detected in this experiment. It is known that spherical pores with cell windows cannot be detected by mercury intrusion, because the mercury has to enter this big pore through a cell window of smaller diameter. With increasing PMMA content, the average pore size and the quantity of mercury intrusion increased, owing to less densification of the

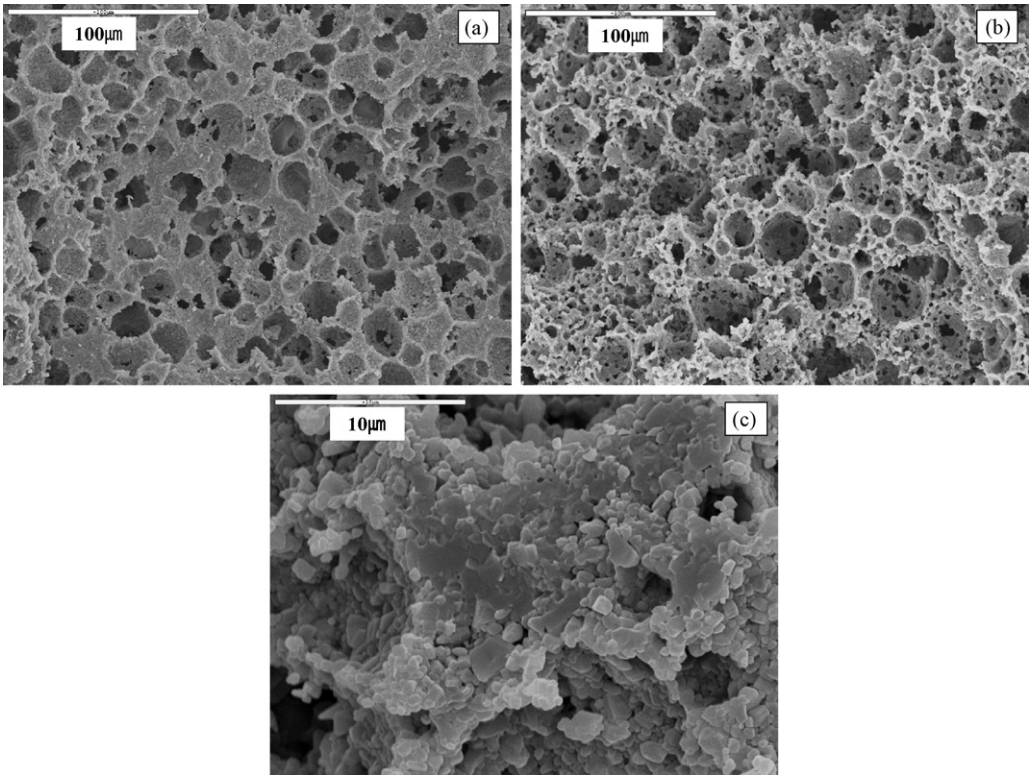

Fig. 4. Typical fracture surfaces of porous SiC ceramics sintered at 1850 °C for 3 h: (a) P0 (0 wt% PMMA), (b) P2 (20 wt% PMMA), and (c) higher magnification of P2.

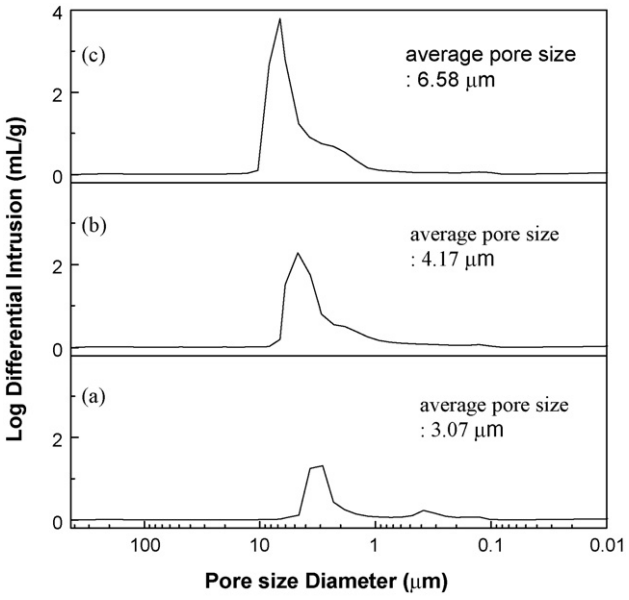

Fig. 5. Pore size distribution of porous SiC ceramics sintered at 1850 °C for 3 h: (a) P0 (0 wt% PMMA), (b) P1 (10 wt% PMMA), and (c) P2 (20 wt% PMMA).

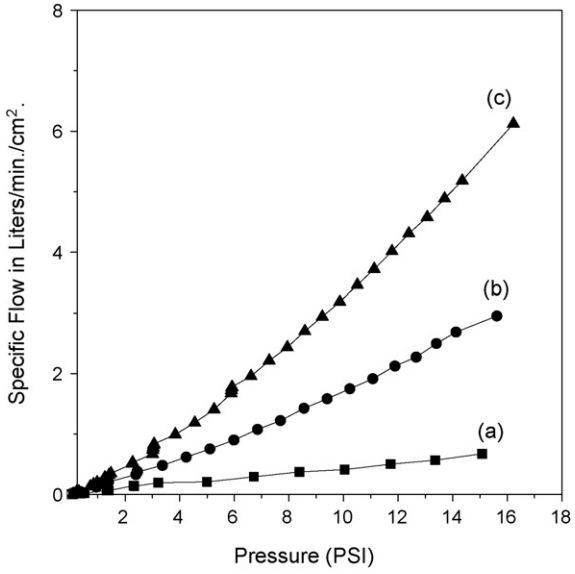

Fig. 6. Air permeability of porous SiC ceramics sintered at 1850 °C for 3 h: (a) P0 (0 wt% PMMA), (b) P1 (10 wt% PMMA), and (c) P2 (20 wt% PMMA).

strut during sintering. The result indicates that open porosity in the strut area increased with increasing PMMA content.

Fig. 6 shows the permeability of porous SiC ceramics sintered at 1850 °C for 3 h. The flow rate increased with increasing PMMA content. The gas permeability coefficient increased with increasing PMMA content: 0.13×10^{12} m^2 for P0, 0.47×10^{12} m^2 for P1, and 0.82×10^{12} m^2 for P2. The addition of PMMA was very effective in terms of increasing the permeability of porous SiC ceramics. Biasetto et al.[40] showed that the permeability of SiOC microcellular ceramics increased with increasing cell window and cell window size. Likewise, the improved permeability observed in Fig. 6 is attributed to the increased openness of the strut, as evidenced by open porosity (Fig. 3(b)), microstructural observations (Fig. 4) and the pore size distribution (Fig. 5).

4. Conclusions

Porous SiC ceramics with a duplex pore structure were successfully fabricated using two kinds of pore former, expandable microspheres and PMMA spheres, thereby resulting in different pores sizes. The duplex pore structure consisted of large pores derived from the expandable microspheres and small windows in the strut area replicated from the PMMA spheres. The development of the duplex pore structure increased the gas permeability coefficient of the porous SiC ceramics significantly, from 0.13×10^{12} m^2 for porous SiC without PMMA spheres to 0.82×10^{12} m^2 for porous SiC with 20 wt% PMMA spheres. The present results suggest that the openness of the strut area in porous ceramics plays an important role in determining the permeability of porous ceramics, and the openness can be effectively adjusted by adding two kinds of templates, resulting in different sizes.

Acknowledgments

This work was supported by a grant from the Center for Advanced Materials Processing (CAMP) of the 21st Century Frontier R&D Program funded by the Ministry of Commerce, Industry and Energy (MOCIE), Republic of Korea.

References

1. Sepulveda P. Gelcasting foams for porous ceramics. *Am Ceram Soc Bull* 1997;**76**:61–5.
2. Lange FF, Miller KT. Open cell, low-density ceramics fabricated from reticulated polymer substrates. *Adv Ceram Mater* 1987;**2**:827–31.
3. Saggio-Woyansky J, Scott CE, Minnear WP. Processing of porous ceramics. *Am Ceram Soc Bull* 1992;**71**:1674–82.
4. Trimis D, Durst F. Combustion in a porous medium-advances and applications. *Combust Sci Technol* 1996;**121**:153–68.
5. Colombo P, Hellmann JR. Ceramic foam porous ceramic preceramic polymer oxycarbide silicone. *Mater Res Innovat* 2002;**6**:260–72.
6. Colombo P. Engineering porosity in polymer-derived ceramics. *J Eur Ceram Soc* 2008;**28**:1389–95.
7. Nangrejo MR, Edirisinghe MJ. Porosity and strength of silicon carbide foams prepared using preceramic polymers. *J Porous Mater* 2002;**9**:131–40.
8. Bao X, Nangrejo MR, Edirisinghe MJ. Preparation of silicon carbide foams using polymeric precursor solutions. *J Mater Sci* 2000;**35**:4365–72.
9. Luyten J, Thijs I, Vandermeulen W, Mullens S, Wallaeys B, Mortelmans R. Strong ceramic foams from polyurethane templates. *Adv Appl Ceram* 2005;**104**:4–8.
10. Nangrejo MR, Bao XJ, Edirisinghe MJ. Preparation of silicon carbide-silicon nitride composites foams from pre-ceramic polymers. *J Eur Ceram Soc* 2000;**20**:1777–85.
11. Zampieri A, Sieber H, Selvam T, Mabande GTP, Schwieger W, Scheffler F, et al. Biomorphic cellular SiSiC/zeolite ceramic composites from rattan palm to bioinspired structured monoliths for catalysis and sorption. *Adv Mater* 2005;**17**:344–9.
12. Fitzgerald TJ, Mortensen A. Processing of microcellular SiC foams. *J Mater Sci* 1995;**30**:1025–32.
13. Colombo P, Bernardo E. Macro- and micro-cellular porous ceramics from preceramic polymers. *Comp Sci Technol* 2003;**63**:2353–9.

14. Yang HF, Zhang GJ, Kondo N, Ohji T, Kanzaki S. Synthesis of porous Si_3N_4 ceramics with rod-shaped pore structure. *J Am Ceram Soc* 2005;**88**:1030–2.
15. Sun Y, Tan SH, Jiang DL. Synthesis of porous silicon carbide and its catalysis. *J Inorganic Mater* 2003;**18**:830–6.
16. Araki K, Halloran JW. Porous ceramic bodies with interconnected pore channels by a novel freeze casting technique. *J Am Ceram Soc* 2005;**88**:1108–14.
17. Eom JH, Kim YW, Song IH, Kim HD. Processing and properties of polysiloxane-derived porous silicon carbide ceramics using hollow microspheres as templates. *J Eur Ceram Soc* 2008;**28**:1029–35.
18. Chae SH, Kim YW, Song IH, Kim HD, Narisawa M. Porosity control of porous silicon carbide ceramics. *J Eur Ceram Soc* 2009;**29**:2867–72.
19. Sepulveda P, Binner JGP. Processing of cellular ceramics by foaming and *in situ* polymerisation of organic monomers. *J Eur Ceram Soc* 1999;**19**:2059–66.
20. Colombo P, Modesti M. Silicon oxycarbide ceramic foams from a preceramic polymer. *J Am Ceram Soc* 1999;**82**:573–8.
21. Zeschkya J, Goetz-Neunhoeffer F, Neubauer J, Jason LSH, Kummer B, Scheffler M, et al. Preceramic polymer derived cellular ceramics. *Comp Sci Technol* 2003;**63**:2361–70.
22. Colombo P, Griffoni M, Modesti M. Ceramic foams from a preceramic polymer and polyurethanes: preparation and morphological characterization. *J Sol–Gel Sci Technol* 1998;**13**:195–9.
23. Colombo P, Modesti M. Silicon oxycarbide foams from a silicone preceramic polymer and polyurethane. *J Sol–Gel Sci Technol* 1999;**14**:103–11.
24. Colombo P. Novel processing of silicon oxycarbide ceramic foams. *Adv Eng Mater* 1999;**1**:203–5.
25. Takahashi T, Colombo P. SiOC ceramic foams through melt foaming of a methylsilicone preceramic polymer. *J Porous Mater* 2003;**10**:113–21.
26. Garrn I, Reetz C, Brandes N, Kroh LW, Schubert H. Clot-forming: the use of proteins as binders for producing ceramic foams. *J Eur Ceram Soc* 2004;**24**:579–87.
27. Kim Y-W, Park CB. Processing of microcellular preceramics using carbon dioxide. *Comp Sci Technol* 2003;**63**:2371–7.
28. Kim Y-W, Kim SH, Wang C, Park CB. Fabrication of microcellular ceramics using gaseous carbon dioxide. *J Am Ceram Soc* 2003;**86**:2231–3.
29. Kim Y-W, Kim SH, Kim HD, Park CB. Processing of closed-cell silicon oxycarbide foams from a preceramic polymer. *J Mater Sci* 2004;**39**:5647–52.
30. Kim Y-W, Kim SH, Song IH, Kim HD, Park CB. Fabrication of open-cell, microcellular silicon carbide ceramics by carbothermal reduction. *J Am Ceram Soc* 2005;**88**:2949–51.
31. Colombo P, Bernardo E, Biasetto L. Novel microcellular ceramics from a silicone resin. *J Am Ceram Soc* 2004;**87**:152–4.
32. Kim Y-W, Jin YJ, Chun YS, Song IH, Kim HD. A simple pressing route to closed-cell microcellular ceramics. *Scripta Mater* 2005;**53**:921–5.
33. Passalacqua E, Freni S, Barone F. Alkali resistance of tape-cast SiC porous ceramic membranes. *Mater Lett* 1998;**34**:257–62.
34. Zhu X, Jiang D, Tan S. Preparation of silicon carbide reticulated porous ceramics. *Mater Sci Eng A* 2002;**323**:232–8.
35. Kitaoka S, Matsushima Y, Chen C, Awaji H. Thermal cyclic fatigue behavior of porous ceramics for gas cleaning. *J Am Ceram Soc* 2004;**87**:906–13.
36. Suwanmethanond V, Goo E, Liu PKT, Johnston G, Sahimi M, Tsotsis TT. Porous silicon carbide sintered substrates for high-temperature membranes. *Ind Eng Chem Res* 2000;**39**:3264–71.
37. Ishizaki K, Komarneni S, Nanko K. *Porous materials; process technology and applications*. London: Kluwer Academic Publisher; 1998 p. 202–24.
38. Eom JH, Kim Y-W, Song IH, Kim HD. Microstructure and properties of porous silicon carbide ceramics fabricated by carbothermal reduction and subsequent sintering process. *Mater Sci Eng A* 2007;**464**:129–34.
39. Ko SI, Lee SJ, Roh MH, Kim W, Kim Y-W. Effect of annealing on mechanical properties of silicon carbide sintered with aluminum nitride and scandium oxide. *Met Mater Int* 2009;**15**:149–53.
40. Biasetto L, Colombo P, Innocentini MDM, Mullens S. Gas permeability of microcellular ceramic foams. *Ind Eng Chem Res* 2007;**46**:3366–72.